INTERNATIONAL JOURNAL FOR NUMERICAL AND ANALYTICAL METHODS IN GEOMECHANICS
Int. J. Numer. Anal. Meth. Geomech. 2011; **35**:406–418
Published online 23 March 2010 in Wiley Online Library (wileyonlinelibrary.com). DOI: 10.1002/nag.902

A three-point time discretization technique for parabolic partial differential equations

A. Khoshghalb[1], N. Khalili[1,*,†] and A. P. S. Selvadurai[2]

[1]*School of Civil and Environmental Engineering, The University of New South Wales, Sydney 2052, Australia*
[2]*Department of Civil Engineering and Applied Mechanics, McGill University, Montreal, QC, Canada H3A 2K6*

SUMMARY

The Crank–Nicolson scheme has second-order accuracy, but often leads to oscillations affecting numerical stability. On the other hand, the implicit scheme is free from oscillation, but it has only first-order accuracy. In this work, a three-point discretization scheme with variable time step is presented for the time marching of parabolic partial differential equations. The method proposed has second-order accuracy, is unconditionally stable and dampens spurious oscillations of the numerical results. The application and effectiveness of the new method are demonstrated through several numerical examples. It is shown that, unlike the Crank–Nicolson method, the approach proposed produces no oscillatory response irrespective of the time step adopted. Copyright © 2010 John Wiley & Sons, Ltd.

Received 17 October 2009; Accepted 11 January 2010

KEY WORDS: stability; parabolic partial differential equations; time discretization

INTRODUCTION

Time marching schemes for the numerical analysis of transient partial differential equations have been studied by many researchers and the most common methods used are forward difference, Crank–Nicolson, Galerkin and backward difference schemes. Among these, the Crank–Nicolson has second-order accuracy, but oscillations of the numerical results usually affect the numerical stability [1].

Wood and Lewis [2] investigated three finite difference techniques for eliminating noise for time integration of the transient heat conduction problem. They concluded that the method of averaging with Crank–Nicolson is an effective way of dealing with noise and provides accurate and stable results, although very small time steps were still troublesome. Vermeer and Verruijt [3] examined the finite element solution for one-dimensional consolidation and established a lower limit for the time step, below which oscillations occurred. Rank *et al.* [4] also showed that for the heat conduction problem small time steps may cause instability, which might lead to physically inadmissible results. They derived the minimum time step for the case of a one-dimensional parabolic partial differential equation based on the discrete maximum principle. Murti *et al.* [5] and Thomas and Zhou [6, 7] extended the Vermeer and Verruijt [3] and Rank *et al.* [4] criteria to two-dimensional problems adapted to different element types. Later, Yang and Gu [8] derived minimum time step criteria for the Galerkin finite element method applied to one-dimensional parabolic partial differential equations, considering the discretization error of a numerical solution. Borja [9]

*Correspondence to: N. Khalili, School of Civil and Environmental Engineering, The University of New South Wales, Sydney 2052, Australia.
†E-mail: n.khalili@unsw.edu.au

investigated the numerical solution of the elastoplastic consolidation problem using the generalized trapezoidal and linear multistep methods based on the backward differentiation formulas. It was shown that the second-order backward differentiation method possesses the potential for usefulness in routine applications; however, more investigations are required before higher order methods can be used in practice. Mohtar and Segerlind [10–12] presented problem-specific time step estimates for using finite elements that captured the influence of the number of nodes in the grid and the problem boundary conditions.

The main objective of this paper is to introduce a generalized, unconditionally stable, oscillation free, second-order accuracy, three-point finite difference technique for the time domain analysis of parabolic partial differential equations. Details of the approach, along with the stability and accuracy analyses and the application of the technique to three simple yet conceptually important transient field problems are presented. Comparisons are made with solutions obtained using the conventional two-point time discretization techniques. It is shown that the method proposed is unconditionally stable with superior accuracy of the numerical results irrespective of the time step adopted.

GOVERNING EQUATIONS

Many time-dependant field problems, such as consolidation, heat conduction, and molecular diffusion, are governed by parabolic partial differential equations

$$\frac{\partial u}{\partial t} = c\nabla^2 u, \tag{1}$$

in which u is an unknown field variable (function of the time and space), c is the diffusion model coefficient, ∇^2 is Laplace's operator, and t is the time. The weak, spatially discretized form of (1) can in turn be written as

$$\boldsymbol{D}\boldsymbol{u} + \frac{\partial \boldsymbol{u}}{\partial t} = 0, \tag{2}$$

where $\boldsymbol{D}$ is a positive-definite property matrix of the system and $\boldsymbol{u}$ denotes the column vector whose elements are the spatial nodal values of the field variable (vectors and matrices are denoted in a bold face throughout). Using the standard Galerkin procedure, $\boldsymbol{D}$ is evaluated as

$$\boldsymbol{D} = \boldsymbol{M}^{-1}\boldsymbol{K}, \tag{3}$$

with $\boldsymbol{K} = \int_V (\nabla \boldsymbol{N})^{\mathrm{T}} c (\nabla \boldsymbol{N})\, \mathrm{d}V$, and $\boldsymbol{M} = \int_V \boldsymbol{N}^{\mathrm{T}} \boldsymbol{N}\, \mathrm{d}V$ in which $\boldsymbol{N}$ is the shape function vector, V is the region of interest and ∇ is the gradient operator. Equation (2) represents a system of first-order differential equations to be discretized in the time domain. To solve this system numerically, the time period of analysis is subdivided into a number of increments. Then, a time marching scheme is employed. The time domain solution of (2) is the main focus of this paper.

TWO-POINT TIME MARCHING SCHEME

In the two-point time marching scheme, having determined the nodal values at time t (mth time level), Equation (2) at time $t+\theta\Delta t$ (time level $m+\theta$) may be written as (see Figure 1(a))

$$\boldsymbol{D}\boldsymbol{u}^{(m+\theta)} + \left(\frac{\partial \boldsymbol{u}}{\partial t}\right)^{(m+\theta)} = 0, \tag{4}$$

where the parameter θ is a time-weighting factor ($0 \leqslant \theta \leqslant 1$) and the superscript inside the parenthesis denotes the time level. Assuming that over the time increment Δt (i.e. from t to $t+\Delta t$) the nodal values vary linearly, $\boldsymbol{u}$ at time level $m+\theta$ is evaluated as (Figure 1(b))

$$\boldsymbol{u}^{(m+\theta)} = (1-\theta)\boldsymbol{u}^{(m)} + \theta \boldsymbol{u}^{(m+1)}. \tag{5}$$

DOI: 10.1002/nag

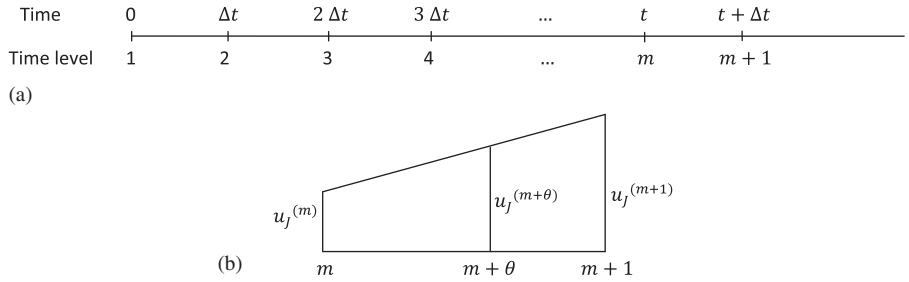

Figure 1. (a) Temporal discretization and (b) evaluation of $u_J^{(m+\theta)}$.

With the two-point finite difference approximation, the time derivative is replaced by

$$\left(\frac{\partial \boldsymbol{u}}{\partial t}\right)^{(m+\theta)} = \frac{\boldsymbol{u}^{(m+1)} - \boldsymbol{u}^{(m)}}{\Delta t}. \tag{6}$$

Substituting (5) and (6) into (4) then yields

$$(\boldsymbol{I} + \Delta t\theta \boldsymbol{D})\boldsymbol{u}^{(m+1)} = (\boldsymbol{I} - \Delta t(1-\theta)\boldsymbol{D})\boldsymbol{u}^{(m)}, \tag{7}$$

where $\boldsymbol{I}$ denotes the identity matrix. It is proven that the value of θ has an important influence on the stability as well as the accuracy of the numerical method. $\theta = 0$ indicates forward interpolation, $\theta = \frac{1}{2}$ represents the Crank–Nicolson method, $\theta = \frac{2}{3}$ corresponds to the Galerkin method, and $\theta = 1$ indicates backward interpolation.

Stability and accuracy

The stability and accuracy of the two-point scheme are well established in the literature. However, a brief discussion is presented here for the sake of completeness.

Let vector $\boldsymbol{u}^{(m)}$ be divided into a correct part $\boldsymbol{u}_c^{(m)}$ and an error term $\boldsymbol{u}_e^{(m)}$, that is,

$$\boldsymbol{u}^{(m)} = \boldsymbol{u}_c^{(m)} + \boldsymbol{u}_e^{(m)}. \tag{8}$$

Therefore, the error at the time level $m+1$ can be obtained from the error at the time level m based on the following recurring equation

$$(\boldsymbol{I} + \Delta t\theta \boldsymbol{D})\boldsymbol{u}_e^{(m+1)} = (\boldsymbol{I} - \Delta t(1-\theta)\boldsymbol{D})\boldsymbol{u}_e^{(m)}. \tag{9}$$

Let $\bar{\boldsymbol{u}}_I$ be the eigenvectors of $\boldsymbol{D}$ with the corresponding eigenvalues $\bar{\lambda}_I$, that is $\boldsymbol{D}\bar{\boldsymbol{u}}_I = \bar{\lambda}_I \bar{\boldsymbol{u}}_I$; thus, the error part of the solution to (7) at the mth time level can be written as

$$\boldsymbol{u}_e^{(m)} = \sum_{I=1}^{N} \rho_I^m \bar{\boldsymbol{u}}_I, \quad m \geqslant 1, \tag{10}$$

where N is the number of nodes in the discretized space and ρ_I are unknown amplification factors. Now, we find ρ_I such that Equation (10) is the solution of Equation (9). Substituting $\boldsymbol{u}_e^{(m)}$ from (10) into (9) and using the correspondence between eigenvalues and eigenvectors, we have

$$\rho_I = \frac{1 - \Delta t(1-\theta)\bar{\lambda}_I}{1 + \Delta t\theta\bar{\lambda}_I}. \tag{11}$$

The method is stable if $|\rho_I| < 1$ in (11), or

$$\theta > \frac{1}{2} - \frac{1}{\Delta t\bar{\lambda}_I}. \tag{12}$$

DOI: 10.1002/nag

Hence, the two-point marching scheme is unconditionally stable for $\frac{1}{2}\leqslant\theta\leqslant 1$. Furthermore, provided $0\leqslant\rho<1$, there will be no oscillation in the numerical solutions by the recursive error term of Equation (10). For the Crank–Nicolson method

$$\rho_I=\frac{1-\frac{1}{2}\Delta t\bar{\lambda}_I}{1-\frac{1}{2}\Delta t\bar{\lambda}_I}. \tag{13}$$

In this case, the Crank–Nicolson method produces oscillations unless $\Delta t<2/\bar{\lambda}_{\max}$ [2]. There is also a lower bound limit for the time step magnitude below that physically unreasonable results will be obtained using the Crank–Nicolson method [3, 5, 8].

THREE-POINT TIME MARCHING SCHEME

In the three-point discretization technique, the time derivative of an arbitrary function, $y(t)$, at time $t+\alpha\Delta t$ is estimated based on the information at time levels $m-1$, m, and $m+1$ (e.g. Figure 2) as

$$\left(\frac{\mathrm{d}y}{\mathrm{d}t}\right)^{(m+1)}\approx\frac{Ay^{(m+1)}+By^{(m)}+Cy^{(m-1)}}{\Delta t}, \tag{14}$$

in which Δt is the time increment between levels $m-1$ and m, α ($\alpha\geqslant 1$) is the time step growth factor, and A, B, and C are the discretization coefficients. In practical applications, it is usually desirable to increase the time steps in the course of the numerical process to increase the computational efficiency without loss of accuracy.

To determine the coefficients A, B, and C, we write a Taylor expansion series of $y(t)$ at time levels m and $m-1$ about time level $m+1$ as

$$y^{(m)}=y^{(m+1)}-\alpha\Delta t\left(\frac{\mathrm{d}y}{\mathrm{d}t}\right)^{(m+1)}+\frac{1}{2}(\alpha\Delta t)^2\left(\frac{\mathrm{d}^2y}{\mathrm{d}t^2}\right)^{(m+1)}+O(\Delta t^3), \tag{15}$$

$$y^{(m-1)}=y^{(m+1)}-(1+\alpha)\Delta t\left(\frac{\mathrm{d}y}{\mathrm{d}t}\right)^{(m+1)}+\frac{1}{2}((1+\alpha)\Delta t)^2\left(\frac{\mathrm{d}^2y}{\mathrm{d}t^2}\right)^{(m+1)}+O(\Delta t^3), \tag{16}$$

where $O(\Delta t^n)$ denotes the nth order accuracy. Substituting (15) and (16) into (14) yields

$$\left(\frac{\mathrm{d}y}{\mathrm{d}t}\right)^{(m+t)}\approx\frac{1}{\Delta t}\left(Ay^{(m+1)}+B\left(y^{(m+1)}-\alpha\Delta t\left(\frac{\mathrm{d}y}{\mathrm{d}t}\right)^{(m+1)}+\frac{1}{2}(\alpha\Delta t)^2\left(\frac{d^2y}{\mathrm{d}t^2}\right)^{(m+1)}+O(\Delta t^3)\right)\right.$$
$$\left.+C\left(y^{(m+1)}-(1+\alpha)\Delta t\left(\frac{\mathrm{d}y}{\mathrm{d}t}\right)^{(m+1)}+\frac{1}{2}((1+\alpha)\Delta t)^2\left(\frac{d^2y}{\mathrm{d}t^2}\right)^{(m+1)}+O(\Delta t^3)\right)\right), \tag{17}$$

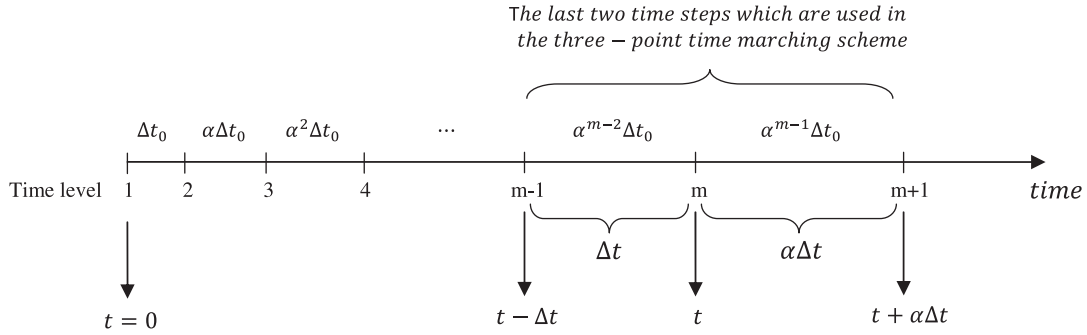

Figure 2. Temporal discretization of the generalized three-point time marching scheme.

DOI: 10.1002/nag

or

$$A+B+C=0, \quad -\alpha B-(1+\alpha)C=1, \tag{18}$$

and, to retain the second-order accuracy for all values of α,

$$(1+\alpha)^2 C+\alpha^2 B=0. \tag{19}$$

Solving (18) and (19) simultaneously yields

$$A=\frac{2\alpha+1}{\alpha(\alpha+1)}, \quad B=-\frac{\alpha+1}{\alpha}, \quad C=\frac{1}{B}. \tag{20}$$

Substitution of (14) into (2) at time $t+\alpha\Delta t$ gives

$$(\Delta t\boldsymbol{D}+A\boldsymbol{I})\boldsymbol{u}^{(m+1)}+B\boldsymbol{u}^{(m)}+C\boldsymbol{u}^{(m-1)}=0, \quad m\geqslant 1, \tag{21}$$

where $\boldsymbol{I}$ is the identity matrix. Having quantified $\boldsymbol{u}$ at all field nodes for the last two time levels (times t and $t-\Delta t$), Equation (21) can be solved to find the nodal values at time $t+\alpha\Delta t$. The solution can then proceed by marching in time.

Stability and accuracy

To examine the stability and accuracy of the proposed three-point time discretization technique, we again divide the vector $\boldsymbol{u}^{(m)}$ into a correct part $\boldsymbol{u}_c^{(m)}$ and an error term $\boldsymbol{u}_e^{(m)}$. The error at the time level $m+1$ is then obtained from the errors at the time levels m and $m-1$ as

$$(\Delta t\boldsymbol{D}+A\boldsymbol{I})\boldsymbol{u}_e^{(m+1)}+B\boldsymbol{u}_e^{(m)}+C\boldsymbol{u}_e^{(m-1)}=0, \quad m\geqslant 1. \tag{22}$$

Again, assuming $\boldsymbol{D}$ has a complete set of orthogonal eigenvectors $\bar{\boldsymbol{u}}_I$ with corresponding eigenvalues $\bar{\lambda}_I$, the solution to Equation (22) at the mth time level may be written as

$$\boldsymbol{u}_e^{(m)}=\sum_{I=1}^{N}\rho_I^m\bar{\boldsymbol{u}}_I, \quad m\geqslant 1, \tag{23}$$

where N is the number of nodes in the discretized space and ρ_I are the amplification factors. Now, we find ρ_I such that Equation (23) can be the solution of Equation (22). Combining (23) and (22), we have

$$\sum_{I=1}^{N}((\Delta t\bar{\lambda}_I+A)\rho_I^{m+1}+B\rho_I^m+C\rho_I^{m-1})\bar{\boldsymbol{u}}_I=0, \quad m\geqslant 1, \tag{24}$$

or

$$(\Delta t\bar{\lambda}_I+A)\rho_I^2+B\rho_I+C=0. \tag{25}$$

The two roots of (25) are

$$\rho_I^{\pm}=\frac{-B\pm\sqrt{B^2-4C(\Delta t\bar{\lambda}_I+A)}}{2(\Delta t\bar{\lambda}_I+A)}. \tag{26}$$

Since (22) is a linear and homogeneous equation, any linear combination arising from the two solutions (26) is also a solution of (22). Therefore, the general form of the error term at the mth time level is written as

$$\boldsymbol{u}_e^{(m)}=\sum_{I=1}^{N}E_I(\rho_I^+)^m\bar{\boldsymbol{u}}_I+\sum_{I=1}^{N}F_I(\rho_I^-)^m\bar{\boldsymbol{u}}_I, \tag{27}$$

DOI: 10.1002/nag

where N is the total number of nodes in the discretized space, E_I and F_I are arbitrary coefficients and $\rho_I^{\pm}$ are the two roots of the second-order equation corresponding to the Ith eigenvector, that is

$$\rho_I^{\pm} = \frac{-B \pm \sqrt{P}\sqrt{1 - Q\Delta t\bar{\lambda}_I}}{2(\Delta t\bar{\lambda}_I + A)}, \quad I = 1, 2, \ldots, N, \tag{28}$$

with $P = B^2 - 4AC$ and $Q = 4C/P$.

Now, if $\Delta t\bar{\lambda}_I > 1/Q$, which occurs at large time steps, $\rho_I^{\pm}$ are complex, yet

$$|\rho_I^{\pm}| = \frac{\sqrt{B^2 + P(Q\Delta t\bar{\lambda}_I - 1)}}{2(\Delta t\bar{\lambda}_I + A)} = \sqrt{\frac{C}{\Delta t\bar{\lambda}_I + A}} < \sqrt{\frac{C}{A}} = \frac{\alpha}{\sqrt{2\alpha + 1}}. \tag{29}$$

It follows that with $1 \leqslant \alpha < 1 + \sqrt{2}$, we always have $0 < |\rho_I^{\pm}| < 1$.

On the other hand, if $\Delta t\bar{\lambda}_I \leqslant 1/Q$, which occurs at small time steps, $\rho_I^{\pm}$ are real. In this case, it is evident that $\rho_I^{+} > 0$, and as we also have $\Delta t\bar{\lambda}_I > 0$ (note that $\boldsymbol{D}$ is positive definite), the positive root in (28) takes the form

$$\begin{aligned} \rho_I^{+} &= \frac{-B + \sqrt{P}\sqrt{1 - Q\Delta t\bar{\lambda}_I}}{2(\Delta t\bar{\lambda}_I + A)} < \frac{-B + \sqrt{P}\sqrt{1 - Q\Delta t\bar{\lambda}_I + \frac{1}{4}Q^2(\Delta t\bar{\lambda}_I)^2}}{2(\Delta t\bar{\lambda}_I + A)} \\ &= \frac{-B + \sqrt{P}\left(1 - \frac{1}{2}Q\Delta t\bar{\lambda}_I\right)}{2(\Delta t\bar{\lambda}_I + A)}. \end{aligned} \tag{30}$$

The right-hand side term of (30) is always less than one, or $\rho_I^{+} < 1$; see Appendix A for details. For the second term of (27), since $B > 1$ and $P < 1$ (for $1 \leqslant \alpha < 1 + \sqrt{2}$), then $\rho_I^{-} > 0$, and

$$\rho_I^{-} = \frac{-B - \sqrt{P}\sqrt{1 - Q\Delta t\bar{\lambda}_I}}{2(\Delta t\bar{\lambda}_I + A)} < \frac{-B}{2A} < 1. \tag{31}$$

In general, provided the growth factor is maintained between the limits $1 \leqslant \alpha < 1 + \sqrt{2}$, then $0 < |\rho_I^{\pm}| < 1$ holds for all values of Δt and $\bar{\lambda}_I$. Hence, the solution is stable and errors tend to vanish as time elapses. Furthermore, $0 < |\rho_I^{\pm}| < 1$ implies that $(\rho_I^{\pm})^m$ tends to zero monotonously with time and causes no oscillation in the numerical results. Thus, the method is unconditionally stable, suppresses spurious oscillations, and has second-order accuracy. Because the three-point time marching scheme employs the results of the two previous time levels, the first step increment cannot be solved using this method and a two-point time marching scheme should be employed. In this study, the backward interpolation method is used to achieve the results for the first step.

APPLICATION

Pumping well fully penetrating a confined aquifer

To illustrate the application of the proposed three-point scheme and to compare its numerical results with the two-point time marching schemes (Crank–Nicolson and fully implicit), the drawdown regime for a pumping well of radius $r_w = 0.1\,\text{m}$, with a constant flow rate, that fully penetrates an axially symmetric confined aquifer was considered. The specific storage and permeability of the aquifer was taken as $S = 0.000184\,\text{m}^{-1}$ and $k = 1090\,\text{m/day}$, respectively, leading to a model coefficient of $c = 5.92 \times 10^6\,\text{m}^2/\text{day}$. A unit thickness of the aquifer was modeled using an axisymmetric mesh, based on four node isoparametric finite elements, as shown in Figure 3. The starting radial dimension of the elements was 0.002 m and increased by a growth factor of

DOI: 10.1002/nag

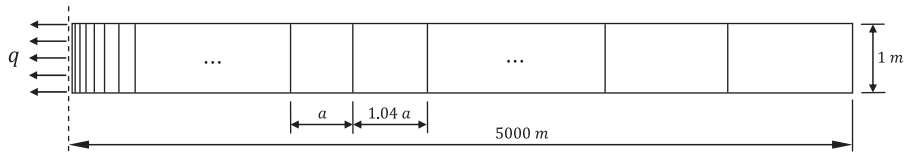

Figure 3. Pumping well fully penetrating a confined aquifer—Mesh (not to scale).

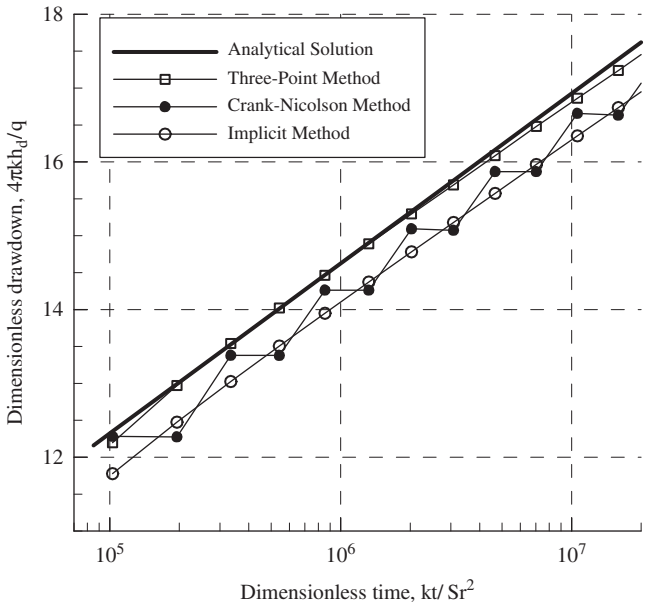

Figure 4. Dimensionless well drawdown versus dimensionless time ($\Delta t_0 = 0.1$ min, $\alpha = 1.5$).

1.04 through the subsequent elements. Twenty-four elements were used. The radial extent of the aquifer was taken as $r_e = 5000$ m. The flow rate of the pumping well per unit thickness of the aquifer was $q = 2500\,\mathrm{m}^2/\mathrm{day}$. The boundary of the region, except at the well bore, was assumed to be impermeable.

The results of the analyses in terms of dimensionless time (kt/Sr^2) versus dimensionless well drawdown ($4\pi kh_d/q$) are shown in Figure 4 (h_d stands for the well drawdown). The initial time step adopted in the analysis was $\Delta t = 0.1$ min, equivalent to the dimensionless time step $\Delta t_D = 41138.3$. The time step growth factor was chosen as $\alpha = 1.5$. As shown, in Figure 4, the Crank–Nicolson method is associated with spurious oscillations that cause a severe degradation in accuracy. It can be seen that the oscillations are not necessarily centered around the exact solution [13], thus the averaging of the values of the oscillatory numerical results cannot be used as a means of accommodating the oscillation problem. The fully implicit method is free from oscillation; however, this method has only one order of accuracy and, therefore, the relative error is appreciable. The three-point scheme is clearly more accurate than both the Crank–Nicolson method and the implicit method, and it also successfully eliminates any oscillation of the numerical solutions.

The same pumping well problem was solved using a coarser time discretization. In this case, the initial time step adopted was $\Delta t = 0.5$ min, equivalent to the dimensionless time step $\Delta t_D = 205690$. The time step growth factor adopted was $\alpha = 2.0$. The results of the analyses are illustrated in Figure 5. Once again, despite using a relatively large time step, there is a good agreement between the analytical solution and the numerical results of the presented scheme. In addition, no tendency for oscillatory results is observed.

DOI: 10.1002/nag

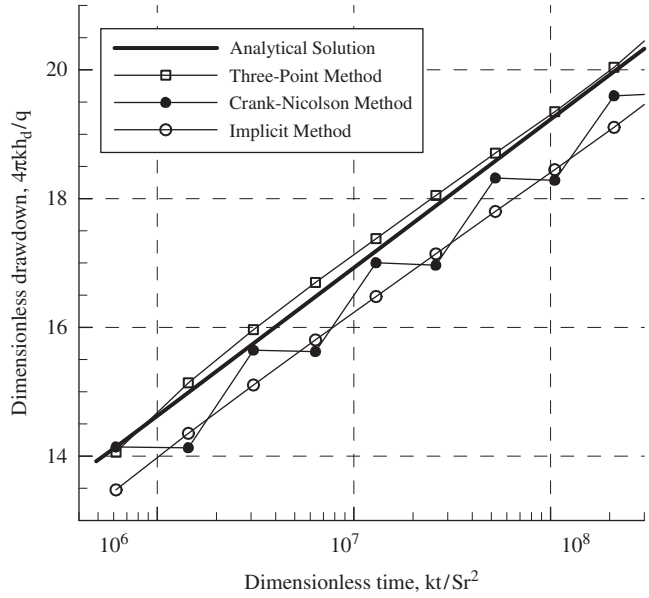

Figure 5. Dimensionless well drawdown versus dimensionless time ($\Delta t_0 = 0.5$ min, $\alpha = 2.0$).

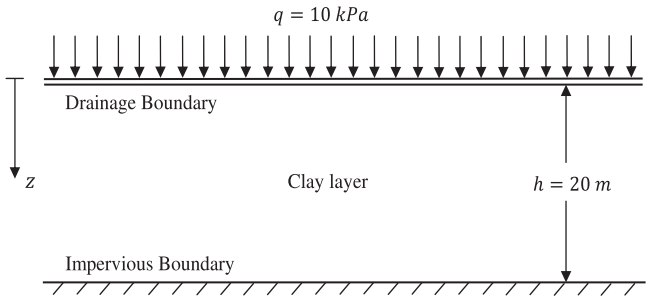

Figure 6. Terzaghi's one-dimensional consolidation problem.

One-dimensional consolidation

In the second example, Terzaghi's problem of one-dimensional consolidation was analyzed. A schematic of the geometry of the problem is shown in Figure 6. The soil layer was assumed to have a thickness of $h = 20$ m. The top surface was fully drained and the bottom surface was rigid and impermeable. The left and right sides of the domain were fixed against horizontal displacement. The model parameter used in the analysis, often referred to as the coefficient of consolidation, was $c = 15\,\mathrm{m}^2/\mathrm{day}$. The applied surcharge at the upper surface was $q = 10$ kPa.

A one-dimensional column of the problem was considered in the analysis. Discretization was achieved using a regular mesh consists of 20 four-node isoparametric elements. The time step discretization used in the analysis was the initial time step of $\Delta t = 0.5$ day and $\alpha = 1.1$.

The numerical results in terms of dimensionless excess pore pressure, p/q, at the depth of $z = 0.05$ h versus dimensionless time, $t_D = ct/h^2$, are given in Figure 7 and compared with the closed-form solution [14].

Again, the Crank–Nicolson method is associated with spurious temporal oscillations that cause a severe degradation in accuracy. The fully implicit method is non-oscillatory; however, it has only one order of accuracy and the errors are discernible, especially at the initial time steps. The three-point scheme, on the other hand, compares exceptionally well with the analytical solution and is oscillation free.

DOI: 10.1002/nag

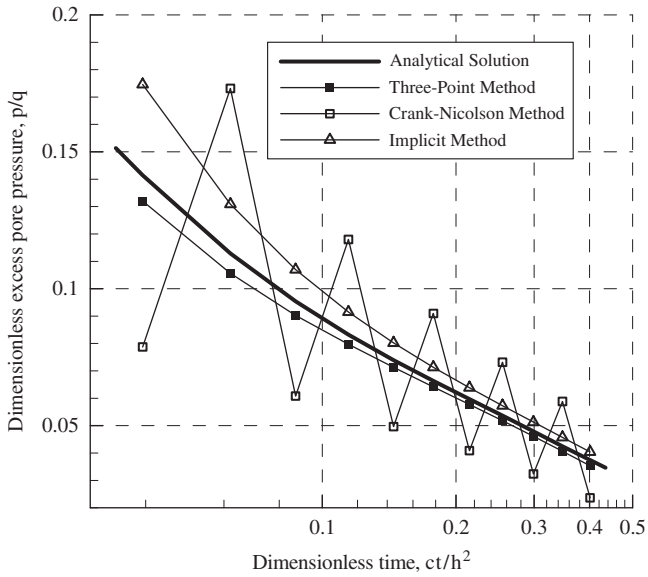

Figure 7. Dissipation of excess pore water pressure at a depth of $z = 0.05\,\mathrm{h}$.

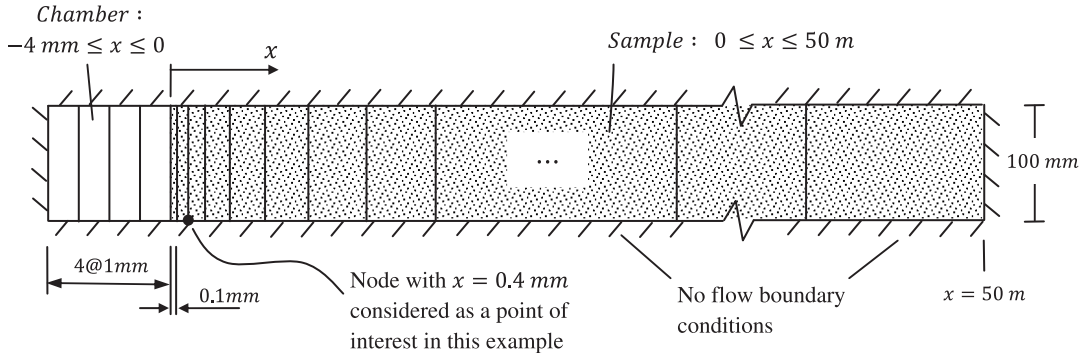

Figure 8. One-dimensional hydraulic pulse test—Mesh (not to scale).

One-dimensional hydraulic pulse test

In this example, the one-dimensional hydraulic pulse test through a semi-infinite column, commonly used in estimating the hydraulic properties of low-permeability saturated porous media, was simulated [15]. The test involves the initial pressurization of water in a solid chamber attached to a low-permeability saturated medium. The time-dependent decay of the fluid pressure within the sample is used as the basis for the computation of the permeability of the specimen.

A 100 mm diameter and 50 m long core of the medium was considered in the analysis (Figure 8). The permeability and specific storage of the medium were $k = 1 \times 10^{-12}\,\mathrm{m/s}$ and $S = 7.67 \times 10^{-7}\,\mathrm{m^{-1}}$, respectively. Accordingly, the model coefficient in this example was $c = 1.3 \times 10^{-6}\,\mathrm{m^2/s}$. The thickness of the solid chamber attached to the core was 4 mm. The compressibility of water in the chamber was $c_w = 4.54 \times 10^{-10}\,\mathrm{Pa^{-1}}$.

The test configuration was modeled using four-node isoparametric finite elements, as shown in Figure 8. The chamber was modeled using four elements of 1 mm width followed by 20 elements for modeling the low-permeability medium. The coordinates of the grid points in the one-dimensional medium in the x direction were 0.1, 0.4, 1, 2, 4, 6, 10, 15, 30, 50, 75, 150, 250, 500, 1000, 2000, 5000, 10 000, 25 000, and 50 000 mm. The boundary of the sample and chamber was impermeable all around. The initial pressure in the chamber was $p_0 = 100\,\mathrm{kPa}$. Defining $\phi = A_c k / \gamma_w V_w c_w$

DOI: 10.1002/nag

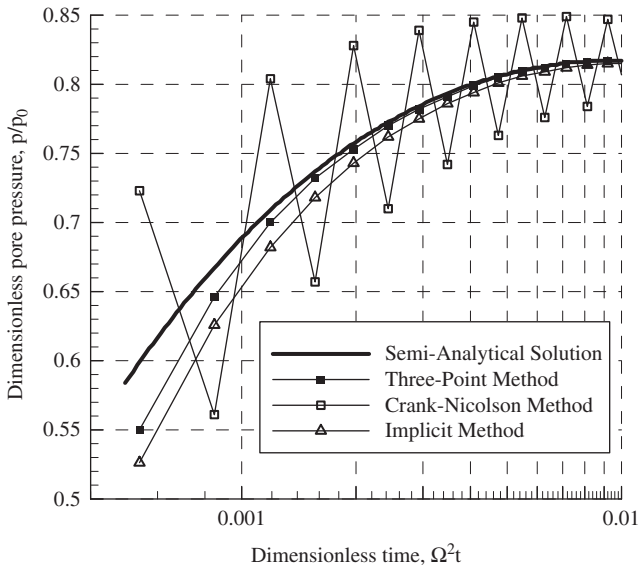

Figure 9. Pore pressure change at $x = 0.4\,\text{mm}$ ($X = 0.0169$) in one-dimensional hydraulic pulse test.

(A_c is the area of the one-dimensional column normal to the direction of flow, V_w is the volume of the chamber, and γ_w is the unit weight of water) and $\Omega^2 = \phi^2/c$, the results of the analyses in terms of dimensionless pore pressure (p/p_0) versus dimensionless time ($\Omega^2 t$) at node $x = 0.4\,\text{mm}$, corresponding to the dimensionless coordinate ($X = (\phi/c)x$) $X = 0.0169$ are shown in Figure 9. Also included in this figure is the graphical representation of the semi-analytical solution to the problem as detailed in Appendix B. The initial time step adopted in the analysis was $\Delta t = 0.11\,\text{s}$, equivalent to the dimensionless time step $\Delta t_D = 2.56 \times 10^{-4}$. The time step growth factor chosen was $\alpha = 1.1$.

As shown, once more the Crank–Nicolson method gives rise to spurious oscillations. There are no oscillations associated with the implicit method, but the method is less accurate than the proposed three-point scheme. On the other hand, the three-point scheme successfully eliminates any oscillations in the numerical solutions and compares well with the semi-analytical solution.

CONCLUSIONS

A three-point time marching scheme with a variable time step has been proposed to increase the efficiency/accuracy of numerical solutions and to suppress the spurious oscillations observed in the time domain analysis of parabolic partial differential equations. Solutions to a transient radial flow problem, one-dimensional consolidation, and a one-dimensional hydraulic pulse test, which itself involves a kinematic time-dependent boundary condition with a time derivative, have been used to demonstrate the accuracy and stability of the proposed technique. Comparisons have also been made with numerical results obtained using the Crank–Nicolson and fully implicit methods. It is shown that the three-point discretization method proposed is superior to the Crank–Nicolson and fully implicit methods from both stability and accuracy points of view. The method also dampens any oscillatory behavior.

APPENDIX A

From the definition of coefficients A, B, and C (20) we have,

$$A = -B - C, \tag{A1}$$

DOI: 10.1002/nag

or

$$B^2+4A^2+4AB=B^2-4AC=P. \tag{A2}$$

Now, since $1\leqslant\alpha<1+\sqrt{2}$, then $2A>B$ and therefore

$$\sqrt{P}-2A-B=0 \quad \overset{P>0 \text{ and } Q>0}{\Longrightarrow} \quad \frac{\sqrt{P}-2A-B}{2+\frac{1}{2}Q\sqrt{P}}=0. \tag{A3}$$

Also noting that $\Delta t\bar{\lambda}_I>0$, we have

$$\Delta t\bar{\lambda}_I>\frac{\sqrt{P}-2A-B}{2+\frac{1}{2}Q\sqrt{P}} \quad \text{or} \quad 2\Delta t\bar{\lambda}_I+2A>-B+\sqrt{P}\left(1-\frac{1}{2}Q\Delta t\bar{\lambda}_I\right), \tag{A4}$$

which yields,

$$\frac{-B+\sqrt{P}\left(1-\frac{1}{2}Q\Delta t\bar{\lambda}_I\right)}{2\Delta t\bar{\lambda}_I+2A}<1. \tag{A5}$$

APPENDIX B

The classical one-dimensional hydraulic pulse test applicable to a semi-infinite domain is governed by the parabolic partial differential equation

$$\frac{\partial p}{\partial t}=c\frac{\partial^2 p}{\partial x^2}, \quad x\in(0,\infty), \tag{B1}$$

subject to the initial condition

$$p(x,0)=0, \quad x\in(0,\infty), \tag{B2}$$

and the boundary conditions

$$p(0,t)=p_0\,\delta(t), \tag{B3}$$

$$\phi\left(-\frac{\partial p}{\partial x}\right)_{x=0}=\left(\frac{\partial p}{\partial t}\right)_{x=0}, \tag{B4}$$

where $\delta(t)$ is the Dirac delta function.

The solution to the problem defined by (B1) to (B4) at $x=0$ can be obtained quite conveniently using a Laplace transform technique as [15]

$$p(0,t)=p_0\exp(\Omega^2 t)\mathrm{Erfc}(\sqrt{\Omega^2 t}), \tag{B5}$$

where Erfc is the complimentary error function defined by

$$\mathrm{Erfc}(\zeta)=1-\int_0^{\zeta}\exp(-\xi^2)\,\mathrm{d}\xi. \tag{B6}$$

In order to determine the time-dependent distribution of pressure within the one-dimensional semi-infinite region, we now consider (B5) as a boundary potential to (B1). Again, using a Laplace

DOI: 10.1002/nag

transform technique it can be shown that the pressure field in the semi-infinite region during the pulse decay is given by

$$p(x,t)=p_0 L^{-1}\left(\frac{\exp\left(-x\sqrt{\frac{s}{c}}\right)}{\sqrt{s}(\sqrt{s}+\Omega)}\right), \tag{B7}$$

where L^{-1} is the inverse Laplace transform. There is no exact closed-form inverse of (B7), expressible in terms of special functions. Hence, the convolution theorem is used to express the inversion in terms of an infinite integral. To aid the development of numerical results in terms of the parameters ϕ and Ω, the partial differential equation is transformed in the non-dimensional form by introducing the variables

$$X=\frac{\phi}{c}x, \quad T=\Omega^2 t, \tag{B8}$$

which reduces (B1) to

$$\frac{\partial^2 p}{\partial X^2}=\frac{\partial p}{\partial T}, \tag{B9}$$

with the boundary condition

$$p(0,t)=p_0\exp(T)\mathrm{Erfc}(\sqrt{T}). \tag{B10}$$

Omitting details of the Laplace transform technique and the application of the convolution theorem, it can be shown that

$$\frac{p(x,t)}{p_0}=\frac{2}{\sqrt{\pi}}\int_{\frac{X}{2\sqrt{T}}}^{\infty}\exp(-\xi^2)\exp\left(T-\frac{X^2}{4\xi^2}\right)\mathrm{Erfc}\left(\sqrt{T-\frac{X^2}{4\xi^2}}\right)\mathrm{d}\xi. \tag{B11}$$

The convergence of the infinite integral is slow but can be evaluated using standard mathematical software, such as MATHEMATICA, MATLAB, or MAPLE. The results shown as a semi-analytical solution in this paper were obtained using this method for the location of interest.

REFERENCES

1. Lawson JD, Morris JL. The extrapolation of first-order methods for parabolic partial differential equations. I. *SIAM Journal on Numerical Analysis* 1978; **15**(6):1212–1224.
2. Wood WL, Lewis RW. Comparison of time marching schemes for the transient heat conduction equation. *International Journal for Numerical Methods in Engineering* 1975; **9**(3):679–689.
3. Vermeer PA, Verruijt A. Accuracy condition for consolidation by finite elements. *International Journal for Numerical and Analytical Methods in Geomechanics* 1981; **5**(1):1–14.
4. Rank E, Katz C, Werner H. On the importance of the discrete maximum principle in transient analysis using finite element methods. *International Journal for Numerical Methods in Engineering* 1983; **19**(12):1771–1782.
5. Murti V, Valliappan S, Khalili-Naghadeh N. Time step constraints in finite element analysis of the Poisson type equation. *Computers and Structures* 1989; **31**(2):269–273.
6. Thomas HR, Zhou Z. Minimum time-step size for diffusion problem in FEM analysis. *International Journal for Numerical Methods in Engineering* 1997; **40**(20):3865–3880.
7. Thomas HR, Zhou Z. Analysis of factors that govern the minimum time step size to be used in the finite element analysis of diffusion problems. *Communications in Numerical Methods in Engineering* 1998; **14**(9):809–819.
8. Yang C, Gu Y. Minimum time-step criteria for the Galerkin finite element methods applied to one-dimensional parabolic partial differential equations. *Numerical Methods for Partial Differential Equations* 2006; **22**(2):259–273.
9. Borja RI. One-step and linear multistep methods for nonlinear consolidation. *Computer Methods in Applied Mechanics and Engineering* 1991; **85**(3):239–272.
10. Mohtar RH, Segerlind LJ. Dynamic time-step estimates for two-dimensional transient field problems using square elements. *International Journal for Numerical Methods in Engineering* 1998; **42**(1):1–14.
11. Mohtar RH, Segerlind LJ. Dynamic time-step estimates for one-dimensional linear transient field problems. *Transactions of the ASAE* 1999; **42**(5):1477–1484.

DOI: 10.1002/nag

12. Mohtar RH, Segerlind LJ. Dynamic time step and stability criteria comparison for the heat diffusion equation. *International Journal of Thermal Sciences* 1999; **38**(6):475–480.
13. Todd DK. *Groundwater Hydrology*. Wiley: New York, 1980; 535.
14. Selvadurai APS. *Partial Differential Equations in Mechanics*, *Volume 1*: *Fundamentals*, *Laplace's Equation*, *Diffusion Equation*, *Wave Equation*. Springer: Berlin, 2000.
15. Selvadurai APS. Influence of residual hydraulic gradients on decay curves for one-dimensional hydraulic pulse tests. *Geophysical Journal International* 2009; **177**(3):1357–1365.

DOI: 10.1002/nag